ARTICLE
Journal of Cellular Biochemistry 106:849–857 (2009)

Journal of Cellular Biochemistry

Differential Expression of Nuclear Matrix Proteins During the Differentiation of Human Neuroblastoma SK-N-SH Cells Induced by Retinoic Acid

Ying Liang, Qi-Fu Li,* Xiu-Yan Zhang, Song-Lin Shi, and Guang-Jun Jing

The Key Laboratory of Education Ministry for Cell Biology and Tumor Cell Engineering, School of Life Sciences, Xiamen University, Xiamen 361005, Fujian Province, PR China

ABSTRACT

To investigate the alteration of nuclear matrix proteins (NMPs) during the differentiation of neuroblastoma SK-N-SH cells induced by retinoic acid (RA), differentiation markers were detected by immunocytochemistry and NMPs were selectively extracted and subjected to two-dimensional gel electrophoresis analysis. Immunocytochemical observation demonstrated that the expression of neuronal markers was up-regulated in SK-N-SH cells following RA treatment. Meanwhile, 52 NMPs (41 of which were identified) changed significantly during SK-N-SH differentiation; four of these NMPs were further confirmed by immunoblotting. This study suggests that the differentiation of neuroblastoma cells was accompanied by the altered expression of neuronal markers and NMPs. The presence of some differentially expressed NMPs was related to the proliferation and differentiation of neuroblastomas. Our results may help to reveal the relationship between NMPs and neuroblastoma carcinogenesis and reversion, as well as elucidate the regulatory principals driving neural cell proliferation and differentiation. J. Cell. Biochem. 106: 849–857, 2009.

KEY WORDS: NUCLEAR MATRIX PROTEINS; DIFFERENTIATION; HUMAN NEUROBLASTOMA; RETINOIC ACID; DIFFERENTIAL EXPRESSION

Neuroblastoma, which is derived from neural crest stem cells, is the most common malignant childhood tumor. It arises in the sympathetic ganglia and adrenal medulla of the sympathetic nervous system [Redlinger et al., 2004]. Research examining neuroblastoma cell differentiation may contribute to the elucidation of the regulatory mechanisms driving cell proliferation and differentiation [Kohler et al., 2000; Lombet et al., 2001]. The nuclear matrix, which is related to DNA replication, mRNA processing, and steroid hormone action, is the filamentous protein framework inside the nucleus. It affects cell division and proliferation by constructing the higher-order architecture of chromatin [Allen et al., 1977; Wunderlich and Herlan, 1977]. The nuclear matrix or nuclear matrix-associated proteins strongly regulate signal transduction and mRNA modification and translation. This is especially true regarding the expression of oncogenes or tumor suppressor genes during the cell cycle and cell differentiation [Marchisio et al., 2005].

The morphology and composition of the nuclear matrix differs in cancer cells and normal cells [Konety and Getzenberg, 1999; Brünagel et al., 2002]. Our early studies showed that nuclear matrix morphology and composition changed distinctively during differentiation of several cell lines treated with different reagents. These results suggested that further study on the expression changes of nuclear matrix proteins (NMPs) during cell differentiation treated with different inducers could reveal the mechanism of carcinogenesis and cancer differentiation. The neuroblastoma line SK-N-SH, established in cell culture from human metastatic neuroblastoma tissue, has been used in neuronal cell-differentiation assays [Pizzi et al., 2002; Chang et al., 2005]. SK-N-SH cells exhibit a neuronal phenotype and express multiple neurochemical markers.

The goal of the present study was to analyze changes in the expression of NMPs during the differentiation of human neuroblastoma SK-N-SH cells induced by retinoic acid (RA). In addition, we sought to identify differentially expressed NMPs related to neuroblastoma cell proliferation and differentiation.

MATERIALS AND METHODS

CELL CULTURE AND TREATMENT

Human neuroblastoma SK-N-SH cells, provided by the China Center for Type Culture Collection (CCTCC), were maintained in RPMI-1640

Grant sponsor: National Natural Science Foundation of China; Grant number: 30470877.

*Correspondence to: Prof. Qi-Fu Li, The Key Laboratory of Education Ministry for Cell Biology and Tumor Cell Engineering, School of Life Sciences, Xiamen University, Xiamen 361005, Fujian Province, PR China.
E-mail: chifulee@xmu.edu.cn

Received 7 August 2008; Accepted 9 December 2008 • DOI 10.1002/jcb.22052 • 2009 Wiley-Liss, Inc.
Published online 21 January 2009 in Wiley InterScience (www.interscience.wiley.com).

medium supplemented with 10% heat-inactivated fetal calf serum, 100 U/ml penicillin, 100 μg/ml streptomycin, and 50 μg/ml kanamycin at 37°C with 5% CO_2 in air. At 24 h after being seeded into dishes, SK-N-SH cells were maintained in culture medium containing 1 μM RA (Sigma) for 7 days to induce differentiation. Meanwhile, SK-N-SH cells were cultured in RPMI-1640 medium as a control. The concentration of RA was determined by pre-experiment evaluating the effects of terminal differentiation on SK-N-SH cells treated with RA. The cells of the control and treatment groups seeded in small culture flasks with cover slip strips were cultured in normal medium and medium containing 1 μM RA, respectively. Medium was replaced every 48 h, and cells were harvested at subconfluency and stored at −80°C.

DETERMINATION OF CELL GROWTH CURVES

SK-N-SH cells collected in the logarithmic phase of growth were suspended to a concentration of 5.0×10^4 cells/ml. At 24 h after seeding, the experimental groups were treated with 1 μM RA, while the control group was continuously cultured in fresh medium. During the first 7 days, untreated or treated cells were harvested from three flasks every 2 days. The number of viable cells was counted three times via the trypan blue dye exclusion test to obtain an average value.

DETERMINATION OF CELL CYCLE

SK-N-SH cells of the treated and control groups were digested, centrifuged at 1,000 rpm for 5 min, and then collected. All cells collected were rinsed in PBS, resuspended, fixed in 70% pre-cooled ethanol at 4°C overnight, centrifuged, and finally resuspended in 20 mg/l RNase A at 37°C for 30 min. Then, 1 mg/l propidium iodide (Sigma) was added to the suspended cells at 4°C in the dark for 30 min. The cell cycle was analyzed by flow cytometry (Becton–Dickinson), and data were analyzed using Cell FIT cell cycle analysis software (version 2.01.2).

SAMPLE PREPARATION FOR LIGHT MICROSCOPY

SK-N-SH cells from the control group and group treated with 1 μM RA for 5 days were seeded in small penicillin bottles with cover slips and grown for 48 h. The cells on cover slips were rinsed with PBS at 37°C, fixed overnight in Bouin–Hollande fixative, stained with hematoxylin–eosin reagents, and observed under a light microscope.

IMMUNOCYTOCHEMICAL ANALYSIS

The cells grown on the cover slips were fixed with cold acetone for 20 min and rinsed twice in PBS for a total of 10 min. They were then immersed in 3% hydrogen peroxide for 10 min, washed with distilled water and PBS successively for a total of 15 min, blocked with 2% BSA for 20 min at room temperature, and incubated with the monoclonal mouse antibodies against human synaptophysin (Syn), NSE, and MAP2 antibodies at 4°C overnight. After washing, secondary antibody incubation was performed with biotin-labeled IgG at 37°C for 10 min, and then incubated in streptavidin–peroxidase at 37°C for 10 min. The antigen–antibody complex was visualized with diaminobenzidine (DAB) substrate. Negative controls were incubated in the absence of primary antibodies.

EXTRACTION OF NMPS

For analysis by two-dimensional polyacrylamide gel electrophoresis (2D PAGE), an extraction method described by Michishita et al. [2002] was used. SK-N-SH cells were washed with ice-cold PBS twice and then extracted by a cytoskeleton (CSK) buffer (100 mM KCl, 3 mM $MgCl_2$, 5 mM EGTA, 10 mM PIPES, pH 6.8, 300 mM sucrose, 0.5% TritonX-100, and 2 mM PMSF) for 10 min at 0°C. After being centrifuged at 1,500 rpm for 5 min, the pellets were washed with ice-cold PBS to remove soluble cytoplasmic proteins. They were then recentrifuged and suspended within the digestion buffer (identical to CSK buffer except with 50 mM NaCl instead of KCl) containing 400 mg/ml DNase I for 30 min at room temperature. Cold ammonium sulfate at a final concentration of 0.25 M was used to terminate the enzyme digestion.

After centrifugation at 3,000 rpm for 10 min, the pellets were washed in CSK buffer and then dissolved in lysis buffer containing 7 M urea, 2 M thiourea, 4% CHAPS, 1.5% Triton X-100, 1% Pharmalyte (pH 3–10, Amersham Biosciences), 65 mM DTT, 40 mM Tris, 5 mg/ml aprotinin, 1 mg/ml leupeptin, 1 mg/ml pepstatin, 2 mM PMSF, and 5 mM EDTA. The sample was sonicated at 0°C for 30 min and centrifuged at 3,000 rpm for 1 h. The protein concentrations of the control and treated supernatants were determined by the Bradford assay, diluted to the same concentration (~5 mg/ml) with lysis buffer, and stored at −80°C.

2D PAGE, MALDI-TOF-MS ANALYSIS AND PROTEIN IDENTIFICATION

Two-dimensional PAGE was performed using standard methods. The gels were stained using a silver nitrate protocol compatible with mass spectrometry. Image scanning (UMAX Power Look III) and analyses (PD Quest 8.0 software, Bio-Rad) of the three triplicate sets of silver-stained 2D gels were performed. After background subtraction, spot detection, and matching of spots from one gel with spots from another gel, spot intensities were obtained by the integration of the Gaussian function with units of intensity calculated as "Intensity * Area as parts per million" (INT*Area PPM). The intensity of each protein spot was normalized to the total intensity of the entire gel. The spots of protein whose intensity changed at least twofold were defined as differentially expressed NMPs.

Spots containing differentially expressed proteins were cut from the gels. After a series of steps including silver removal, reduction with DL-dithiothreitol, alkylation with iodacetamide, and in-gel digestion with trypsin, peptide mass fingerprints (PMFs) were generated using Bruker III MALDI-TOF mass spectrometer. Flex Analysis software was used to analyze the PMF data in order to calibrate and remove polluted peaks. The data were searched against the NCBInr and Swiss-Prot protein databases using the Mascot tool from Matrix Science.

WESTERN BLOTTING

The NMPs and whole-cell proteins were separated by SDS-PAGE and then transferred onto PVDF membranes. Non-specific reactivity was blocked by incubating the membranes at 4°C for 1 h in 2% BSA in PBS. The membranes were incubated with primary antibodies against nucleophosmin, prohibitin, vimentin, and hnRNP A2/B1

(Santa Cruz) overnight at 4°C. After being washed, the secondary antibody (combined with horseradish peroxidase) was used to detect bound primary antibody. Reactive protein was detected using an enhanced chemiluminescence (ECL) detection system (Pierce). Two percent BSA was used in the negative group instead of the primary antibodies. β-actin was also detected as an internal control.

SAMPLE PREPARATION FOR NM-IF SYSTEM

The cells grown on the cover slips were selectively extracted as described by Capco et al. [1982] was used. The cells were rinsed with PBS twice at 37°C, and extracted by high ionic strength extraction solution (10 mM PIPES, pH6.8, 250 mM $(NH_4)_2SO_4$, 300 mM sucrose, 3 mM $MgCl_2$, 1.2 mM PMSF, 0.5% TritonX-100) at 4°C for 3 min. The extracted cells were then rinsed in non-enzyme digestion solution (same as extraction solution except with 50 mM NaCl instead of 250 mM $(NH_4)_2SO_4$), and digested in digestion solution containing DNase I (400 mg/l) and RNase A (400 mg/l) for 20 min at 23°C. After that, the extracted samples were placed in high ionic strength extraction solution at 23°C for 5 min. So far only the nuclear matrix-intermediate filament structure remained intact.

SAMPLE PREPARATION FOR THE FLUORESCENCE MICROSCOPY

The NM-IF samples on the cover slips were prefixed with 4% paraformaldehyde at 4°C for 10 min, blocked with 2% BSA for 1 h at room temperature, and incubated with NPM, PHB, vimentin, and hnRNP A2/B1 primary antibodies (1:200) at 4°C overnight. After washing, the cells were incubated with secondary antibody (1:1,000), which was labeled with fluorescence dye TRITC (red), washed with TBST, and dried by airing. After that, they were enveloped with 90% glycerol and then observed under fluorescence microscopy. The whole process after incubation with secondary antibody should be performed in the dark. Negative controls were incubated in the absence of primary antibodies.

RESULTS

EFFECTS OF RA ON THE PROLIFERATION OF SK-N-SH CELLS

Determination the cell growth curve showed that the proliferation of SK-N-SH cells is extremely fast. On the 7th day, the number of cells in the control and treated groups increased to 29.33×10^4 and 12.34×10^4/ml, respectively; these values are 5.9- and 2.5-fold higher than the original value of 5.0×10^4/ml for each group. The doubling time of the control group was 28.64 h, whereas that of the treated group was 68.07 h. Thus, the growth in the treated group was slowed by 57.9% (Fig. 1A).

The cell cycle of SK-N-SH cells was analyzed by flow cytometry. The results showed that the cell cycle distribution of SK-N-SH cells changed significantly when the cells were treated with RA. In the control group, 49.7% of cells were in the G0/G1 phase, 21.4% were in the S phase, and 27.7% were in the G2/M phase. In the treated group, 62.7% were in the G0/G1 phase, 11.5% were in the S phase, and 22.6% were in the G2/M phase (Fig. 1B).

EFFECTS OF RA ON THE MORPHOLOGY AND EXPRESSION OF NEURONAL MARKERS IN SK-N-SH CELLS

Light microscopy showed that SK-N-SH cells had morphological characteristics typical of malignant human neuroblastoma and similar to those of fibrocyte cells. The overall volume of the SK-N-SH cells was relatively large, nuclei were large and irregular with several nucleoli, and the nucleoplasmic ratio was relatively large (Fig. 2A). In contrast to untreated cells, cells treated with RA underwent a significant morphological change and appeared as normal differentiated neuronal cells: the shape of the nuclei became regular, and cells became thin and bipolar. Seven days later, the treatment produced multipolar and star-shaped cells with short neurites; cell bodies were smaller, with long axonal processes extending from one cell to another to form ganglia (Fig. 2B). In this way, the extent of morphological changes induced by RA depended

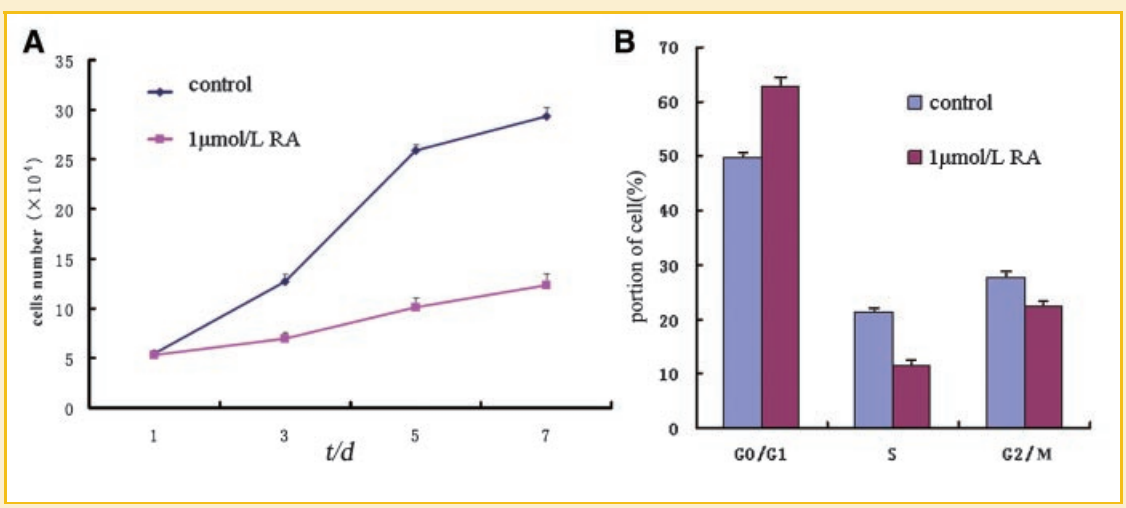

Fig. 1. Effect of RA on the proliferation of SK-N-SH cells. A: Viable cells were counted by the trypan blue dye exclusion test to obtain average value. The growth inhibition rate of SK-N-SH treated with RA was 57.9% on the 7th day ($P < 0.05$). B: The cell cycles of untreated or treated SK-N-SH cells were analyzed by flow cytometry, and data were analyzed with Cell FIT cell cycle analysis software ($P < 0.05$).

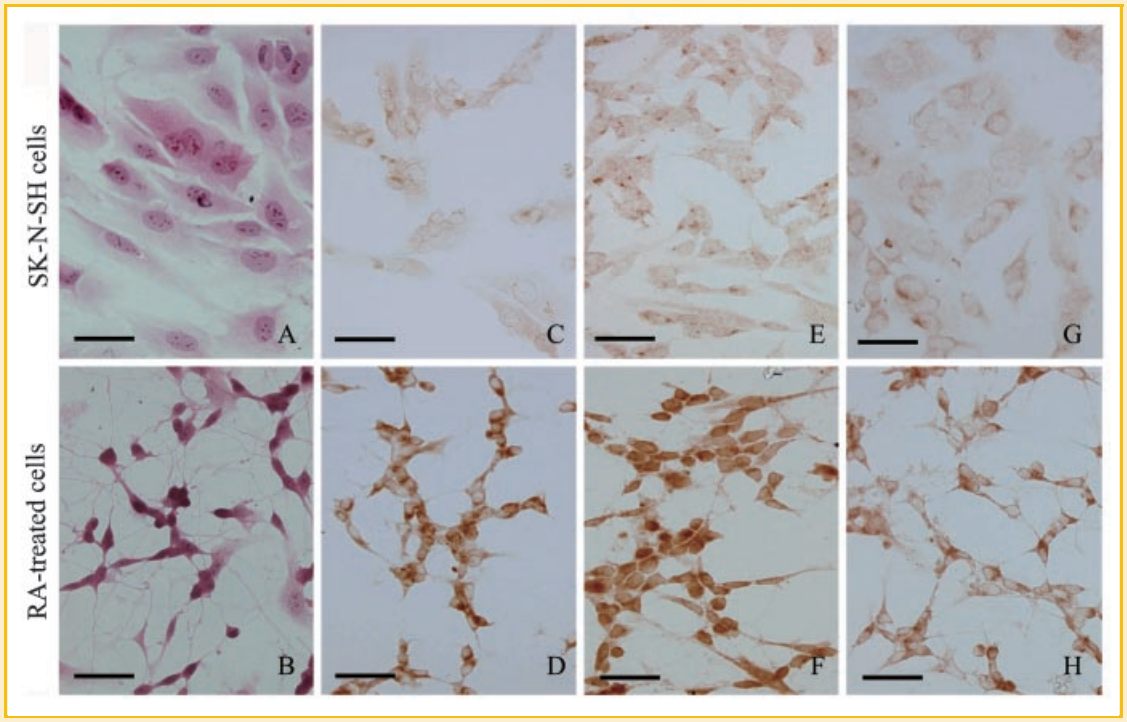

Fig. 2. Light microscope (LM) observation of SK-N-SH cells. Untreated SK-N-SH cells (A) and cells treated with RA (B) were observed by using HE staining. Untreated SK-N-SH cells and cells treated with RA were immunocytochemically stained for synaptophysin (C,D), NSE (E,F), and MAP2 (G,H) (Bar = 20 μm).

on the number of differentiating days. The neuronal phenotype of differentiated SK-N-SH cells was demonstrated by immunocytochemistry using antibodies against the neuronal markers Syn, NSE, and MAP2.

Immunocytochemistry showed that the Syn level in the control group was lower compared to the treated group. Brown–yellow granules were detected in the cytoplasm around the nuclear membrane of SK-N-SH cells and rarely in nuclei (Fig. 2C). After treatment with RA, the expression of Syn was increased. The dark brown–yellow granules were detected mainly in the cytoplasm around the nuclear membrane, but the protein level remained low in nuclei; in fact, brown–yellow particles were rarely detected in nuclei (Fig. 2D).

Immunocytochemistry showed low levels of NSE protein in the control group compared to the treated group; light brown–yellow granules were detected mainly in nucleoli and cytoplasm, whereas the signal was virtually absent in cell nuclei (Fig. 2E). After treatment with RA, the level of NSE protein in SK-N-SH cells increased. The evenly distributed brown granules were detected in nucleoli and cytoplasm. Their distribution was irregular (Fig. 2F).

Immunocytochemistry showed that MAP2 protein level in control group was lower compared to the treated group. The signal in the cytoplasm and cell membrane was very weak. Light brown–yellow granules were detected mainly in the cytoplasm, and no expression was detectable in nuclei (Fig. 2G). After treatment with RA, MAP2 expression increased greatly. Evenly distributed brownish-red granules were mainly detected in marginal areas of the cytoplasm and protuberances of cells, while there were small quantity distributions in nuclei of the cells (Fig. 2H).

RESULTS OF 2D PAGE AND IMAGE ANALYSIS

The NMPs extracted from SK-N-SH cells of the treated group were subjected to 2D PAGE. Quantification of images for three triplicate sets of silver-stained 2D gels was performed using PD Quest 8.0 software (Bio-Rad). The analysis of proteins was based on the evaluation of at least two gels. A total of 52 protein spots changed appreciably. Most spots corresponding to NMPs from differentiated SK-N-SH cells showed similar intensities to those in the control group (Fig. 3A). Most spots concentrated in the area corresponding to pI 4–9, indicating sizes in the range 10–100 kDa. Forty-one NMPs were differentially expressed during the differentiation process. Among the spots whose intensity changed during differentiation, 26 decreased (L1–L26), 3 disappeared (N1–N3), 10 increased (H1–H10), and 2 emerged as new protein spots (N4–N5) in the differentiated SK-N-SH cells. The other 11 spots were not identified because of their low protein abundance or lack of matches to the protein database. The relative expression levels of the changed proteins were shown using Melanie ViewerII software (Fig. 3B,C). The relative abundance (ppm) of spots was used to correct the data for artifactual intensity differences between gels due, for example, to differences in protein loading or staining. These proteins were identified via a search of the Swiss-Prot database (Table I). Additionally, NMPs samples from over five different cell preparations, and there was no significant difference in the level of variation in NMP profiles from one cell preparation to another ($P < 0.05$).

IMMUNOBLOTTING OF THE ALTERED EXPRESSION NMPS

Bands for nucleophosmin (NPM, 38 kDa), prohibitin (PHB, 32 kDa), vimentin (53–55 kDa), and hnRNP A2/B1 (37 kDa) were observed in

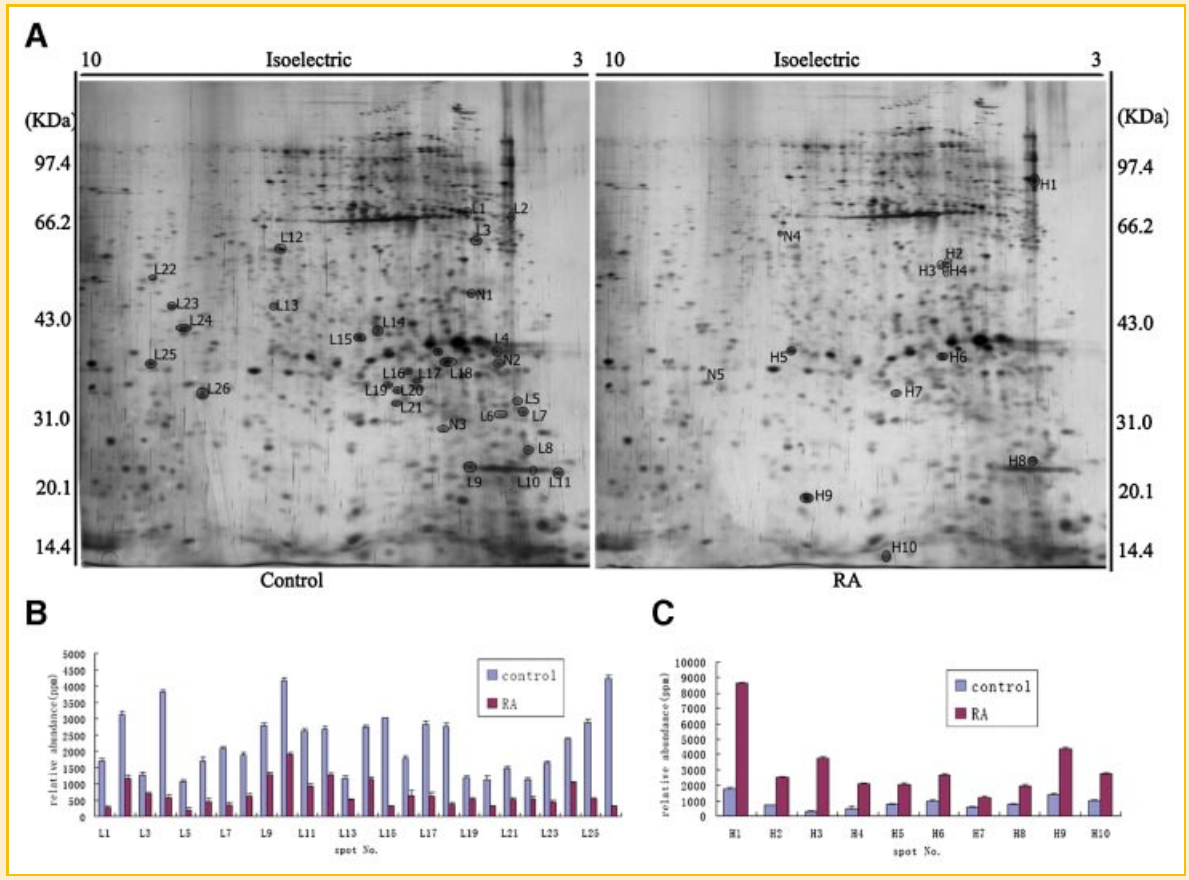

Fig. 3. Two-dimensional protein profiles from the nuclear matrix of SK-N-SH cells. A: Proteins were separated on the basis of pI (X-axis) and molecular mass (Y-axis) and visualized by silver staining. The differentially expressed proteins are shown as circular symbols on the gels. L indicates down-regulated NMPs, and H indicates up-regulated NMPs in SK-N-SH cells treated with RA. B: Relative abundance of down-regulated NMPs in untreated SK-N-SH cells and cells treated with RA ($P < 0.05$). C: Relative abundance of up-regulated NMPs in untreated SK-N-SH cells and cells treated with RA ($P < 0.05$).

NM-IF (nuclear matrix-intermediate filament) (Fig. 4A) and whole-cell proteins (Fig. 4B) samples of control and RA-treated cells. The nucleophosmin, prohibitin, and hnRNP A2/B1 bands detected in control cells were at greater levels than those from RA-treated cells; in contrast, the reverse is true of the vimentin band. These findings suggest that RA treatment down-regulated expression of nucleophosmin, prohibitin, and hnRNP A2/B1, while it strongly up-regulated expression of vimentin protein. All of these Western blotting results are consistent with the results of the 2D PAGE analysis.

The observation of immunofluorescence revealed the localization and expression of nucleophosmin. The results showed that the highly intensified NPM fluorescence mainly distributed in the residual nucleoli region of SK-N-SH cells, while the intensity of fluorescence was very low in the nuclear matrix and lamina regions (Fig. 5A). After treatment with RA, the distribution and expression of NPM altered evidently. The intensity of fluorescence within the nucleus region dropped, especially in the nucleoli region while that in the lamina and karyotheca regions ascended. NPM also displayed the tendency of transferring from nucleoli regions to nuclear matrix. Faint fluorescence could be observed even in the intermediate filaments (Fig. 5B).

The observation of immunofluorescence revealed the localization and expression of prohibitin. The results showed that the red fluorescence of PHB existed in the whole cell, but was relatively weak in regions near to the nuclear membrane. The distribution of red fluorescence was uniform in the cytoplasm region (Fig. 5C). After treatment with RA, the distribution and expression of PHB changed significantly. The holistic intensity of the fluorescence in nuclear matrix and nuclear lamina region dropped; especially there was small quantity distribution in nuclei of the cells (Fig. 5D).

The observation of immunofluorescence revealed the localization and expression of vimentin. The results showed that the red fluorescence of vimentin was weak in nuclei where it scattered as little particles. The distribution of red fluorescence was rarely detected in the cytoplasm region (Fig. 5E). After treatment with RA, the distribution and expression of vimentin also changed significantly. The intensity of the fluorescence in nuclear matrix and intermediate filaments increased greatly, especially in the cytoplasm region (Fig. 5F).

The observation of immunofluorescence revealed the localization and expression of hnRNP A2/B1. The results showed that the red fluorescence of hnRNP A2/B1 was mainly located in the whole nuclear region, whereas the signal was relatively weak in the

TABLE I. Differential Expression of Nuclear Matrix Proteins Were Identified by MS

Spot number	Protein name	Accession number	Mol. mass calc (Da)	pI (calc)	Score/coverage
Down-regulated proteins					
L1	DNA replication licensing factor	Q14566	93,801	5.29	55/13%
L2	IMMT	Q9P0V2	84,025	6.08	66/11%
L3	TRPV2	Q9Y5S1	86,838	5.56	60/10%
L4	Annexin A5	P08758	35,971	4.94	128/32%
L5	Nucleophosmin	Q96EA5	32,726	4.64	73/25%
L6	Nucleophosmin	Q96EA5	32,726	4.64	73/25%
L7	Nucleophosmin	Q96EA5	32,726	4.64	73/25%
L8	Prohibitin	P35232	29,859	5.57	93/37%
L9	Prohibitin	P35232	29,859	5.57	93/37%
L10	Prohibitin	P35232	29,859	5.57	93/37%
L11	RAB-3D	O95716	24,480	4.76	62/31%
L12	GLDH1	P00367	61,701	7.66	106/25%
L13	WISP3	O95389	41,329	8.87	77/29%
L14	tRNA-DUS2	Q9NX74	55,814	6.73	131/26%
L15	FAAA	P16930	46,743	6.46	61/28%
L16	ZFP193	O15535	46,951	6.94	55/15%
L17	Mitosin	P49454	36,736	5.03	54/6%
L18	PCNT	O95613	38,064	5.39	55/11%
L19	ARF5	P84085	20,631	6.30	71/35%
L20	PRPP I	P60891	35,325	6.51	58/21%
L21	RAB-23	Q9ULC3	26,871	6.22	64/32%
L22	Uncharacterized protein	Q9H943	71,463	9.34	60/13%
L23	CDC7-related protein kinase	O00311	64,646	8.96	55/20%
L24	BCKD	O14874	46,616	8.97	58/8%
L25	hnRNP A2/B1	P22626	36,600	8.67	101/43%
L26	CDK 2	P24941	34,079	8.80	78/26%
Up-regulated proteins					
H1	MTMR2	Q13614	73,878	6.83	54/24%
H2	Vimentin	P08670	53,545	5.06	96/18%
H3	Vimentin	P08670	53,545	5.06	96/18%
H4	Vimentin	P08670	53,545	5.06	96/18%
H5	SYAP1	Q96A49	39,966	4.45	53/25%
H6	GFAP	Q9UFDO	49,907	5.42	61/17%
H7	Syntenin-1	O00560	32,595	7.05	58/20%
H8	PEA-15	Q15121	15,088	4.93	55/27%
H9	Protein mago nashi homolog	P61326	17,210	5.74	62/33%
H10	SUMO3	P55854	11,687	5.32	65/25%
Disappear proteins					
N1	ATP synthase beta chain	P06576	59,012	5.26	78/17%
N2	Uncharacterized protein C13 or f3	Q8IX90	46,843	4.99	56/16%
N3	PSB 3	P49720	23,219	6.14	54/23%
Appear proteins					
N4	LGI1	O95970	64,519	8.50	59/14%
N5	SYCE1	Q8NOS2	40,074	5.89	60/21%

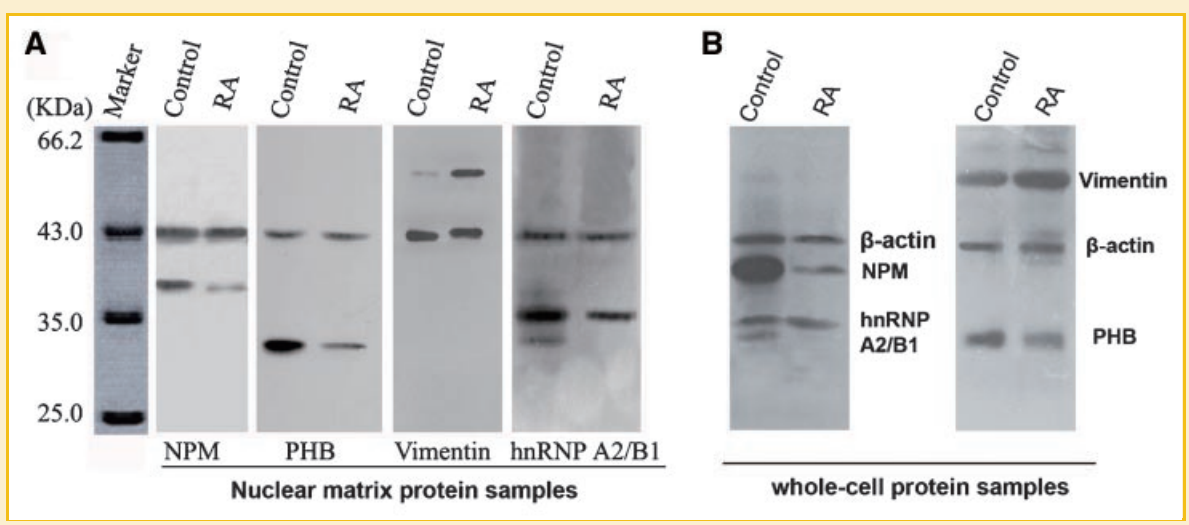

Fig. 4. Confirmation of the differential expression of specific NMPs from NMP samples (A) and whole-cell protein samples (B) by Western blotting. β-actin was used as a protein loading control. The bands were detected by an enhanced chemiluminescence (ECL) detection system. The control is the samples from SK-N-SH cells, and RA is the samples from RA-treated SK-N-SH cells (NPM, nucleophosmin; PHB, prohibitin).

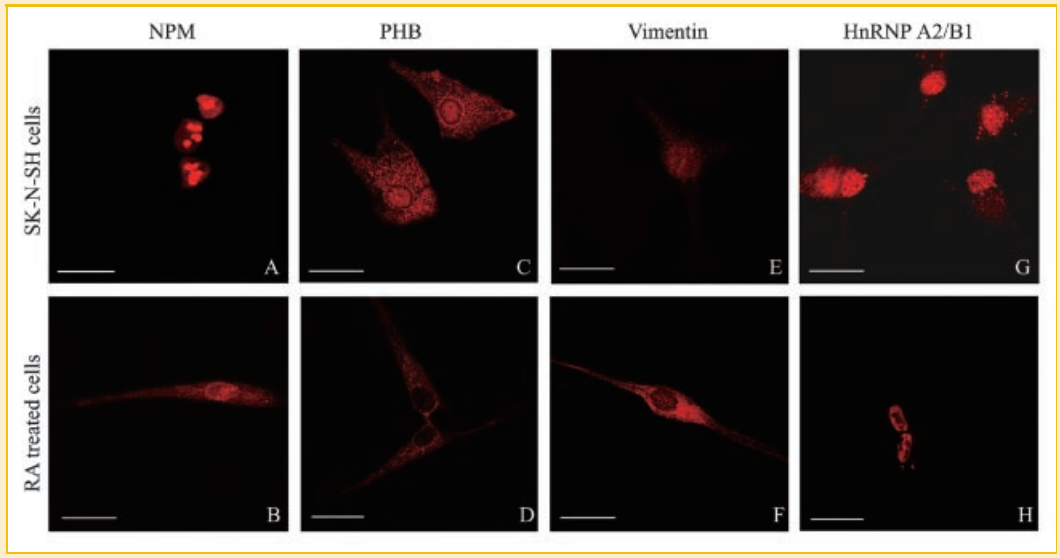

Fig. 5. Observation of localization and expression of the differential expression of specific NMPs in the NM-IF system of SK-N-SH cells and RA-treated cells by fluorescence microscopy. Untreated SK-N-SH cells and cells treated with RA were immunofluorescence stained for NPM (A,B), PHB (C,D), vimentin (E,F), and hnRNP A2/B1 (G,H) (labeled with fluorescence dye TRITC, Bar = 30 μm).

cytoplasm region (Fig. 5G). After treatment with RA, the distribution and expression of hnRNP A2/B1 showed obvious changes. The holistic intensity of the fluorescence in nuclear matrix and nuclear lamina region dropped, and the fluorescence mainly distributed in the nucleus except the nucleoli region (Fig. 5H).

DISCUSSION

Uncontrolled cell proliferation and division are some of the most important characteristics that differentiate normal cells from tumor cells. An important indicator that cells can response to the effects of inducers involves blocking cells progression into the G0/G1 phase. The proliferation of tumor cells provides a significant index for identifying exogenous inducers of differentiation [Shi et al., 2006]. In this study, the cell growth curve and cell cycle indicated that SK-N-SH cells could proliferate vigorously. The cell proliferation of the group treated with RA was inhibited as early as the day after treatment, and these results demonstrate that RA inhibits proliferation of SK-N-SH cells and blocked entry into the G0/G1 phase. The effects of RA on cell growth and the cell cycle here are consistent with its anti-proliferative effects, through cell cycle arrest, reported in human gastric, colonic, and endometrial carcinoma cell lines [Zhang and Chen, 2005]. Our experiments show that RA can effectively inhibit the proliferation of human neuroblastoma SK-N-SH cells, promote the expression of neurochemical markers of differentiation, and induce differentiation of normal nerve cells.

SK-N-SH cells, a neuronal cell line subcloned from human neuroblastoma, can be induced to differentiate. They can be transformed into normal neuronal cells, expressing the proteins normally found only in this type of cell. Changes in cell morphology and markers indicated a change in the status of cell differentiation; in fact, these are two of the most important indicators used to determine the functional status of tumor cells [Li et al., 2006]. Microscopic observation revealed morphological changes in cells treated with RA. Compared with the control group, cells treated with RA developed multipolar and extended neurites similar to axons. Cells fused together to form ganglion-like structures, and the length of the axon-like structures continually increased. Parts of these structures overlapped showing the same phenotype as nerve cells following RA treatment.

Changes in neuronal marker expression play a role in neuroblastoma cell carcinogenesis, reverse movement, and proliferation. The inactivation of associated genes (e.g., Syn, NSE, and MAP2) is the primary indicator of human neuroblastoma cell differentiation [Jain et al., 2007]. Syn, which is distributed in nerve terminals and neuroendocrine tissues, is a synaptic vesicle protein in the pre-synaptic capsule. NSE, which is derived from neurons and neuroendocrine cells, is the main enolase isozyme in the neuron. Microtubule-associated protein 2 (MAP2), which is distributed primarily in neuronal cell bodies and dendrites, is a tubulin structural protein. In this study, the expression levels of Syn, NSE, and MAP2 proteins were low in untreated SK-N-SH cells. Their significant increase in response to RA treatment may promote the expression of neuronal markers. Previous studies have shown that RA up-regulates the expression of neuronal markers, confirming that RA affects the differentiation of SK-N-SH cells [Lombet et al., 2001; Sánchez et al., 2001; Sarkanen et al., 2007].

Abnormalities of the nuclear matrix system are closely associated with the carcinogenic nature of cells [Chen et al., 2007]. Previous studies showed that the nuclear matrix in cancer cells has a distinctive, irregular morphology different from that of normal cells [Nickerson, 1998; Li, 1999]. We further analyzed the alterations of NMPs in order to identify the effects of RA on the differentiation of SK-N-SH cells. The electrophoresis identified 41 NMPs that were differentially expressed during the differentiation process. Previous

studies in other cell lines showed that the composition of the nuclear matrix varies during the different stages of cell differentiation [Zhao and Li, 2005]. Similarly, our own studies confirmed that the HMBA-induced differentiation of the human osteosarcoma cell line MG-63 was accompanied by changes of NMPs [Zhao et al., 2006a]. In the present study, we show for the first time that the levels of specific NMPs change during the differentiation of SK-N-SH cells.

Especially, in our previous studies and the present study, we found that nuclephosmin, prohibitin, hnRNP A2/B1, and vimentin are the common differentially expressed NMPs during the differentiation of different tumor cells induced by the same inducer or the same tumor cell induced by different inducers [Zhao et al., 2006a,b]. The changes of localization and expression of the four proteins in the filaments of nuclear matrix indicate that these altered NMPs have multiple cellular functions associated with tumor promotion as well as tumor suppressor depending on binding partners, cellular location, and cell cycle. Therefore, it could be preliminarily inferred that the four proteins played a very important role in the procedure of differentiation, although many mechanisms have not been investigated because this procedure involves such a complicated regulative network of many other regulators. Further researches on these proteins and their mechanism in the modulation of tumor cell differentiation will be very significant in the more insightful understanding of the anti-tumor mechanism and the induced differentiation mechanism of tumor cells.

Intranuclear informatics can be combined with proteomics and genomics to develop a novel platform for the identification and targeting of regulatory pathways in cancer cells [Zaidi et al., 2007]. More and more research has showed that these identified NMPs are significant not only for their localization in the nucleus or binding to the nuclear matrix, but also because they may influence cell proliferation and differentiation or apoptosis by regulating gene expression at the transcriptional, mRNA processing, and posttranscriptional levels. For example, NPM is dysregulated in human malignancies leading to anti-apoptosis and inhibition of differentiation. Treatment of several different cancer cell types with the inhibitor of NPM resulted in an up-regulation of p53 and induced apoptosis in a dose-dependent manner [Qi et al., 2008]. And evidences showed that inhibiting NPM shuttling in nuclear and cytoplasm could block cellular proliferation [Maggi et al., 2008]. This suggests that the observed down-regulation of nucleophosmin in the RA-treated SK-N-SH cells would in fact be expected. Additionally, it has been observed that PHB is required for full and efficient androgen antagonist-mediated growth suppression of prostate cancer cells; it can repress androgen receptor-mediated transcription and androgen-dependent cell growth [Gamble et al., 2007; Dai et al., 2008]. PHB also appears to be a candidate marker for distinguishing prostate hyperplasia and cancer [Ummanni et al., 2008]. Finally, hnRNP A2/B1 with its splicing variant hnRNP B1 are proteins, which are involved in cellular proliferation, differentiation, and protein synthesis are up-regulated in non-small cell lung cancer [Zech et al., 2006]; and hnRNPA2/B1could link the p53 tumor suppressor to RNA processing [Prahl et al., 2008]. In a word, further characterization of these proteins and their interactions with the nuclear matrix network are important for both revealing the mechanism of carcinogenesis and understanding the phenotypic reversion of tumor cells.

In conclusion, our results demonstrate that RA inhibits proliferation and induces SK-N-SH cells to differentiate. The array of NMPs expressed, follow the SK-N-SH cells changes substantially during differentiation. In fact, our study has identified several NMPs associated with the differentiation of neuroblastoma. Our findings will help to elucidate the signaling pathways and mechanisms of neuroblastoma cell growth and differentiation as well as carcinogenesis. Further study of the proteins identified here will be useful for the development of clinical therapies targeting neuroblastoma.

REFERENCES

Allen SL, Berezney R, Coffey DS. 1977. Phosphorylation of nuclear matrix proteins in isolated regenerating rat liver nuclei. Biochem Biophys Res Commun 75:111–116.

Brünagel G, Vietmeier BN, Bauer AJ, Schoen RE, Getzenberg RH. 2002. Identification of nuclear matrix protein alterations associated with human colon cancer. Cancer Res 62:2437–2442.

Capco DG, Wan KM, Penman S. 1982. The nuclear matrix: Three-dimensional architecture and protein composition. Cell 29:847–858.

Chang PA, Chen R, Wu YJ. 2005. Reduction of neuropathy target esterase does not affect neuronal differentiation, but moderate expression induces neuronal differentiation in human neuroblastoma (SK-N-SH) cell line. Brain Res Mol Brain Res 141:30–38.

Chen LY, Tang J, Xu DH, Niu JW, Li QF. 2007. Configurational changes of the nuclear matrix-intermediate filament (NM-IF) system during the differentiation of human hepatocarcinoma SMMC-7721 cells after being induced by hexcamethylamine bisacetamide (HMBA). J Chin Electron Microsc Soc 26:212–216.

Dai Y, Ngo D, Jacob J, Forman LW, Faller DV. 2008. Prohibitin and the SWI/SNF ATPase subunit BRG1 are required for effective androgen antagonist-mediated transcriptional repression of androgen receptor-regulated genes. Carcinogenesis 29:1725–1733.

Gamble SC, Chotai D, Odontiadis M, Dart DA, Brooke GN, Powell SM, Reebye V, Varela-Carver A, Kawano Y, Waxman J, Bevan CL. 2007. Prohibitin, a protein downregulated by androgens, represses androgen receptor activity. Oncogene 26:1757–1768.

Jain P, Cerone MA, Leblanc AC, Autexier C. 2007. Telomerase and neuronal marker status of differentiated NT2 and SK-N-SH human neuronal cells and primary human neurons. J Neurosci Res 85:83–89.

Kohler JA, Imeson J, Ellershaw C, Lie SO. 2000. A randomized trial of 13-cis retinoic acid in children with advanced neuroblastoma after high-dose therapy. Br J Cancer 83:1124–1127.

Konety BR, Getzenberg RH. 1999. Nuclear structural proteins as biomarkers of cancer. J Cell Biochem 75:183–191.

Li QF. 1999. Effect of retinoic acid on the changes of nuclear matrix-intermediate filament system in gastric carcinoma cells. World J Gastroenterol 5:417–420.

Li QF, Ou Yang GL, Li CY, Hong SG. 2006. Effects of tachyplesin on the morphology and ultrastucture of human gastric carcinoma cell line BGC-823. World J Gastroenterol 6:676–680.

Lombet A, Zujovic V, Kandouz M, Billardon C, Carvajal-Gonzalez S, Gompel A, Rostène W. 2001. Resistance to induced apoptosis in the human neuroblastoma cell line SK-N-SH in relation to neuronal differentiation. Role of Bcl-2 protein family. Eur J Biochem 268:1352–1362.

Maggi LB, Jr., Kuchenruether M, Dadey DY, Schwope RM, Grisendi S, Townsend RR, Pandolfi PP, Weber JD. 2008. Nucleophosmin serves as a

rate-limiting nuclear export chaperone for the mammalian ribosome. Mol Cell Biol 28:7050–7065.

Marchisio M, Santavenere E, Paludi M, Gaspari AR, Lanuti P, Bascelli A, Ercolino E, Baldassarre AD, Miscia S. 2005. Erythroid cell differentiations characterized by nuclear matrix localization and phosphorylation of protein kinases C (PKC) α, δ, ζ. J Cell Physiol 205:32–36.

Michishita E, Kurahashi T, Suzuki T, Fukuda M, Fujii M, Hirano H, Ayusawa D. 2002. Changes in nuclear matrix proteins during the senescence-like phenomenon induced by 5-chlorodeoxyuridine in HeLa cells. Exp Gerontol 37:885–890.

Nickerson JA. 1998. Nuclear dreams: The malignant alteration of nuclear architecture. J Cell Biochem 70:172–180.

Pizzi M, Boroni F, Bianchetti A, Moraitis C, Sarnico I, Benarese M, Goffi F, Valerio A, Spano P. 2002. Expression of functional NR1/NR2B-type NMDA receptors in neuronally differentiated SK-N-SH human cell line. Eur J Neurosci 16:2342–2350.

Prahl M, Vilborg A, Palmberg C, Jornvall H, Asker C, Wiman KG. 2008. The p53 target protein Wig-1 binds hnRNP A2/B1 and RNA helicase A via RNA. FEBS Lett 582:2173–2177.

Qi W, Shakalya K, Stejskal A, Goldman A, Beeck S, Cooke L, Mahadevan D. 2008. NSC348884, a nucleophosmin inhibitor disrupts oligomer formation and induces apoptosis in human cancer cells. Oncogene 27:4210–4220.

Redlinger RE, Mailliard RB, Barksdale EM. 2004. Neuroblastoma and dendritic cell function. Semin Pediatr Surg 13:61–71.

Sánchez C, Arellano JI, Rodríguez-Sánchez P, Avila J, DeFelipe J, Díez-Guerra FJ. 2001. Microtubule-associated protein 2 phosphorylation is decreased in the human epileptic temporal lobe cortex. Neuroscience 107:25–33.

Sarkanen JR, Nykky J, Siikanen J, Selinummi J, Ylikomi T, Jalonen TO. 2007. Cholesterol supports the retinoic acid-induced synaptic vesicle formation in differentiating human SH-SY5Y neuroblastoma cells. J Neurochem 102: 1941–1952.

Shi SL, Wang YY, Liang Y, Li QF. 2006. Effects of tachyplesin and n-sodium butyrate on proliferation and gene expression of human gastric adenocarcinoma cell line BGC-823. World J Gastroenterol 12:1694–1698.

Ummanni R, Junker H, Zimmermann U, Venz S, Teller S, Giebel J, Scharf C, Woenckhaus C, Dombrowski F, Walther R. 2008. Prohibitin identified by proteomic analysis of prostate biopsies distinguishes hyperplasia and cancer. Cancer Lett 266:171–185.

Wunderlich F, Herlan G. 1977. Reversibly contractile nuclear matrix. Its isolation, structure and composition. J Cell Biol 73:271–278.

Zaidi SK, Young DW, Javed A, Pratap J, Montecino M, van Wijnen AJ, Lian JB, Stein JL, Stein GS. 2007. Nuclear microenvironments in biological control and cancer. Nat Rev Cancer 7:454–463.

Zech VF, Dlaska M, Tzankov A, Hilbe W. 2006. Prognostic and diagnostic relevance of hnRNP A2/B1, hnRNP B1 and S100 A2 in non-small cell lung cancer. Cancer Detect Prev 30:395–402.

Zhang HC, Chen XM. 2005. Research development in children solid tumor differentiation by retinoic acid. Med Recapitulate 11:616–619.

Zhao CH, Li QF. 2005. Altered profiles of nuclear matrix proteins during the differentiation of human gastric mucous adenocarcinoma MGc80-3 cells. World J Gastroenterol 11:4628–4633.

Zhao CH, Li QF, Zhao Y, Niu JW, Li ZX, Chen JA. 2006a. Changes of nuclear matrix proteins following the differentiation of human osteosarcoma MG-63 cells. Genomics Proteomics Bioinformatics 4:10–17.

Zhao Y, Tang J, Zhao CH, Shi SL, Li QF. 2006b. Observation of the effects of retinoic acid on the configurational changes of the NM-IF system and the alteration of nuclear matrix proteins in human osteosarcoma cell line MG-63. J Xiamen Univ (Nat Sci) 45:6–10.